AN EXPONENTIAL TIME-DIFFERENCING METHOD FOR MONOTONIC RELAXATION SYSTEMS

PEDER KRISTIAN AURSAND[A], STEINAR EVJE[B], TORE FLÅTTEN[C], KNUT ERIK TEIGEN GILJARHUS[C] AND SVEND TOLLAK MUNKEJORD[C,D]

Abstract. We consider stiff relaxation processes, emphasizing the application to hyperbolic conservation laws. We present first and second-order accurate exponential time-differencing methods for systems of monotonic relaxation ODEs. Some desirable accuracy and robustness properties of these methods are established.

Through operator splitting, we show how the methods may be applied to hyperbolic conservation laws with relaxation terms. In particular, global second-order accuracy for smooth solutions may be achieved through Strang splitting and MUSCL interpolation. An application to granular-gas flow is presented.

subject classification. 65L04, 65L06, 65M08, 76T25

key words. exponential integrators, relaxation, granular gases

1. Introduction

We are interested in numerical methods for hyperbolic relaxation systems in the form

$$\frac{\partial \boldsymbol{U}}{\partial t} + \frac{\partial \boldsymbol{F}(\boldsymbol{U})}{\partial x} = \frac{1}{\epsilon}\boldsymbol{R}(\boldsymbol{U}), \tag{1}$$

to be solved for the unknown M-vector $\boldsymbol{U}$. Herein, $\boldsymbol{R}(\boldsymbol{U})$ is a *relaxation source term*, the effect of which is to drive the system towards some local equilibrium value $\boldsymbol{U}^{\mathrm{eq}}$. The parameter ϵ represents a characteristic *relaxation time* towards equilibrium. This relaxation time is typically small, imposing a high degree of stiffness in the system (1).

Such systems were extensively analysed by Chen et al. [4], with a particular focus on the stiff limit $\epsilon \to 0$. In this paper, we investigate numerical methods suitable for systems in the form (1) for nonzero, yet small values of ϵ. In particular, we will use *fractional-step* methods, based on splitting the system (1) into two parts:

(i) The conservation law

$$\frac{\partial \boldsymbol{U}}{\partial t} + \frac{\partial}{\partial x}\boldsymbol{F}(\boldsymbol{U}) = 0; \tag{2a}$$

Date: March 28, 2011.

[A]Dept. of Physics, Norwegian University of Science and Technology (NTNU), NO-7491 Trondheim, Norway.

[B]Dept. of Petroleum Engineering, University of Stavanger (UiS), NO-4036 Stavanger, Norway.

[C]SINTEF Energy Research, P.O. Box 4761 Sluppen, NO-7465 Trondheim, Norway.

Email: pederka@pvv.org, steinar.evje@uis.no, Tore.Flatten@sintef.no, Knut.Erik.Giljarhus@sintef.no, stm@pvv.org.

[D]Corresponding author.

(ii) The ordinary differential equation

$$\frac{\mathrm{d}\boldsymbol{U}}{\mathrm{d}t} = \frac{1}{\epsilon}\boldsymbol{R}(\boldsymbol{U}). \tag{2b}$$

This allows for applying methods that are particularly tailored to such problems individually. In particular, we here focus on methods particularly suited for relaxation models in the form (2b).

Recently, a popular approach towards solving stiff systems in the form (2b) has been the use of *exponential integrators* [5, 11, 17]. Such methods are motivated mainly by computational efficiency considerations [12]; without sacrificing high-order accuracy, one gets rid of the severe restriction on the time step commonly associated with explicit methods for stiff problems. The main idea behind such methods consists of splitting the source term into a linear and a nonlinear part as follows:

$$\frac{1}{\epsilon}\boldsymbol{R}(\boldsymbol{U}) = \boldsymbol{L}\boldsymbol{U} + \boldsymbol{N}(\boldsymbol{U}), \tag{3}$$

where $\boldsymbol{L}$ is a constant $M \times M$ matrix. One then attempts to associate the stiffness of the system (2b) with the linear part, which may be solved exactly through the matrix exponential. Coupled to this, the non-linear part $\boldsymbol{N}(\boldsymbol{U})$ is solved by standard Runge–Kutta methods.

In this paper, we wish to emphasize another aspect of exponential time-differencing methods; the potential for strong robustness in the sense that the numerical solution is bounded with no restriction on the time step. In particular, one may use such methods to ensure that the relaxation step does not introduce unphysical solutions such as vacuum or negative-density states.

To achieve this, we here present what seems to us a slightly original twist to the idea of exponential integrators. Instead of viewing the exponential integration step as the *exact* solution to a linear sub-problem as given by the splitting (3), we interpret the exponential integration as a *numerical approximation* to the original nonlinear problem, and this approximation is nevertheless accurate to a certain order in the time step. This change of perspective leads to a slightly different formulation, and allows us to construct consistent methods that *by design* guarantee that the equilibrium solution cannot be exceeded.

For consistency, the property that the numerical solution is bounded by the equilibrium value must be shared by the mathematical solution. Therefore, we will limit our investigations in this paper to what we denote as *monotonic* equations in the relaxation step (2b), as defined more precisely in Section 3. This restricts the class of systems where our methods are applicable, but in particular includes many relaxation processes of interest within the context of (1).

Furthermore, as the solution of such hyperbolic relaxation systems tend to remain close to the equilibrium state, we are interested in deriving methods that exhibit a particularly high level of accuracy near equilibrium. In these respects, the methods investigated in this paper may be particularly well suited for systems in the form (1).

However, the investigations in this paper are in many ways preliminary. In particular, our analysis is limited to the relaxation step (2b). We do not formally address the convergence of our splitting method when applied to the full system (1). Hence, the purpose of this paper may be summarized as follows.

- We wish to emphasize the potential robustness properties of exponential methods. Towards this aim, we explicitly present first and second-order methods possessing a strong form of stability, which we will denote as *monotonic asymptotic* stability.
- We wish to demonstrate the practical feasibility of such methods by applying them to a benchmark case previously investigated in the literature.

By this, we hope to pave the way for further work.

This paper is organized as follows. In Section 2, we briefly review hyperbolic relaxation systems in the form (1), and some existing numerical methods to solve such systems. In Section 3, we present the exponential integration technique which is the topic of this paper. First and second-order versions are provided. We also prove the following.

(i) The methods are stable in the strong sense that no numerical overshoots of the equilibrium value are possible.
(ii) The methods are accurate in the sense that they correspond to the exact solution to first-order deviations from the equilibrium.

In Section 4, we describe a granular-gas model investigated by Serna and Marquina [27]. In Section 5, we present some numerical examples. Herein, Section 5.2 details our numerical method as applied to the granular-gas model. The simulations indicate that our proposed method compares satisfactorily to results previously reported in the literature.

Finally, in Section 6 we summarize our results and discuss some directions for further work.

2. Hyperbolic Relaxation Systems

A hyperbolic relaxation system can be written in general quasilinear form as follows [21]:

$$\frac{\partial \boldsymbol{U}}{\partial t} + \boldsymbol{A}(\boldsymbol{U})\frac{\partial \boldsymbol{U}}{\partial x} = \frac{1}{\epsilon}\boldsymbol{R}(\boldsymbol{U}), \tag{4}$$

where the matrix $\boldsymbol{A}$ is assumed to be diagonalizable with real eigenvalues in the domain of interest. In the context of (1), $\boldsymbol{A}$ is given by

$$\boldsymbol{A}(\boldsymbol{U}) = \frac{\partial \boldsymbol{F}}{\partial \boldsymbol{U}}. \tag{5}$$

Such systems model many relevant physical problems, such as two-phase flows which are locally not in thermodynamic equilibrium [7, 8, 26, 31].

The limiting process $\epsilon \to 0$ in systems in the form (4) was extensively analysed by Liu [19] and Chen et al. [4], with a particular focus on the relationship between stability and wave propagation. In this paper, we are interested in *numerical methods* for systems in the form (4) when the relaxation source term is stiff; i.e. the parameter ϵ is so small that the time scales associated with the homogeneous system (2a) are significantly larger than the time scales associated with the relaxation terms (2b).

Several approaches have been proposed in the literature. These may be roughly divided into *splitting* and *unsplit* methods [23].

2.1. **Fractional-Step Methods.** We assume a uniform computational grid, and let $\boldsymbol{U}_j^n$ denote the cell averages of $\boldsymbol{U}$ in the cell $[x_{j-1/2}, x_{j+1/2}]$ at time t^n. Let $\mathcal{H}(t)$ be the operator that advances the system (2a) forward in time, and let $\mathcal{S}(t)$ be the corresponding stiff ODE operator for the system (2b). Then we may consider two main classes of splitting methods [14]:

- *Godunov splitting*:

$$\boldsymbol{U}^{n+1} = \mathcal{S}\left(\Delta t\right) \circ \mathcal{H}\left(\Delta t\right) \boldsymbol{U}^n, \tag{6}$$

- *Strang splitting* [28]:

$$\boldsymbol{U}^{n+1} = \mathcal{H}\left(\frac{1}{2}\Delta t\right) \circ \mathcal{S}\left(\Delta t\right) \circ \mathcal{H}\left(\frac{1}{2}\Delta t\right) \boldsymbol{U}^n. \tag{7}$$

Godunov splitting is first-order accurate, whereas Strang splitting is second-order accurate provided that both $\mathcal{H}$ and $\mathcal{S}$ are second-order accurate operators. In particular, Strang splitting applied to (2a)–(2b) is second-order accurate for any fixed ϵ. However, as emphasized by Pareschi and Russo [23], and proved by Jin [15], the method in general degenerates to first order in the limit $\epsilon \to 0$. Although this limit may never be fully realized in practical applications, this is nevertheless an undesirable property. Following the terminology of [23], we will denote schemes that retain their order of accuracy also in the limit $\epsilon \to 0$ as *asymptotically accurate*.

Jin [15] proposed an asymptotically second-order accurate splitting method based on two-stage Runge–Kutta time integration. This paved the way for a currently popular class of methods; implicit-explicit (IMEX) Runge–Kutta methods [2, 3, 23] where an explicit discretization is applied to the flux terms and an implicit one to the source terms. This provides a general framework for achieving high-order asymptotic accuracy.

In this paper however, we are interested in exploring robust *explicit* methods for the relaxation source terms. For simplicity, we will remain in the framework of the Godunov and Strang splittings described above. For the hyperbolic operator $\mathcal{H}$, we will use the MUSTA method of Toro [29], augmented with the MUSCL approach of van Leer [30]. Our stiff operator $\mathcal{S}$ will be described in the following section.

3. Monotonically Asymptotic Exponential Integration

In general, relaxation processes in the form (2b) only affect some of the variables of the full system. Furthermore, the relaxation processes often represent an exchange of a conserved property between two variables, for which the relaxation source term will differ only in sign.

This situation allows us to fully express the solution vector $\boldsymbol{U}$ through the dynamics of a *reduced* variable $\boldsymbol{V}(\boldsymbol{U})$, with rank $N < M$. For the purposes of this paper, we make the following definition.

Definition 1. *Consider the equation*

$$\frac{\mathrm{d}\boldsymbol{V}}{\mathrm{d}t} = \frac{1}{\epsilon}\boldsymbol{S}(\boldsymbol{V}), \qquad \boldsymbol{V} \in \mathcal{D} \subseteq \mathbb{R}^N \tag{8}$$

where $\boldsymbol{S}(\boldsymbol{V})$ is a smooth function. The system is said to be a **relaxation ODE** *provided there exists a unique point $\boldsymbol{V}^{\mathrm{eq}} \in \mathcal{D}$ such that $\boldsymbol{S}(\boldsymbol{V}^{\mathrm{eq}}) = 0$, and the solution satisfies*

$$\lim_{t\to\infty} \boldsymbol{V}(t) = \boldsymbol{V}^{\mathrm{eq}}. \tag{9}$$

Herein, the initial condition $\boldsymbol{U}_0$ of (2b) determines an invertible function $\boldsymbol{V}(\boldsymbol{U})$, as well as the function $\boldsymbol{S}(\boldsymbol{V})$ and the point $\boldsymbol{V}^{\mathrm{eq}}$. This will be illustrated by an explicit example in Section 4.2.

3.1. **Monotonic Relaxation ODEs.** One way of solving relaxation ODEs is by using *exponential integrators*, an idea that dates back at least several decades [6, 18]. A common starting point for such methods is a splitting of the source term into a linear and a nonlinear part as follows [1, 5, 12, 13]:

$$\frac{1}{\epsilon}\boldsymbol{S}(\boldsymbol{V}) = \boldsymbol{L}\boldsymbol{V} + \boldsymbol{N}(\boldsymbol{V}), \tag{10}$$

where $\boldsymbol{L}$ is a constant $N \times N$ matrix. The linear part may then be solved exactly through the matrix exponential of $\boldsymbol{L}$; this solution is then coupled to the nonlinear part $\boldsymbol{N}(\boldsymbol{V})$ through standard Runge–Kutta methods.

For stiff problems, exponential integrators allow for larger time steps and improved stability compared to straightforward Runge–Kutta methods. Berland et al. [1] presented a general theory for constructing higher-order versions of such exponential integrators.

Much of the literature focuses on computational *accuracy* and *efficiency*. In our current paper, we wish to shift the focus more strongly towards numerical *robustness*. Towards this end, we first define a subclass of relaxation ODEs.

Definition 2. *A relaxation ODE in the form* (8) *is said to be a* **monotonic relaxation ODE** *if*

$$V_i'(t)\,(V_i^{\mathrm{eq}} - V_i) > 0 \quad \forall V_i \neq V_i^{\mathrm{eq}} \tag{11}$$

for all $i \in \{1, \ldots, N\}$.

In other words, we denote the system as monotonic if all the components of the solution vector are monotonic functions of time. From (8) and (11) we immediately see that a *necessary* condition for a system in the form (8) to be a monotonic relaxation ODE is that the source term must satisfy

$$S_i(\boldsymbol{V})\,(V_i^{\mathrm{eq}} - V_i) > 0 \quad \forall V_i \neq V_i^{\mathrm{eq}} \tag{12}$$

for all $i \in \{1, \ldots, N\}$.

Within the framework of hyperbolic relaxation systems in the form (1), monotonicity seems to be a rather inclusive restriction. For instance, it is an essential property of scalar relaxation ODEs.

Proposition 1. *All scalar relaxation ODEs are monotonic, and a scalar ODE in the form* (8) *is a relaxation ODE if and only if there is a point* V^{eq} *such that*

$$[\min(V_0, V^{\mathrm{eq}}), \max(V_0, V^{\mathrm{eq}})] \subseteq \mathcal{D} \tag{13}$$

and

$$\begin{gathered} S(V)\,(V^{\mathrm{eq}} - V) > 0 \quad \forall V \neq V^{\mathrm{eq}}, \\ S(V^{\mathrm{eq}}) = 0. \end{gathered} \tag{14}$$

Proof. Either all scalar relaxation ODEs are monotonic, or some orbit of V exists where $V'(t)$ changes sign. However, given that $S(V)$ is a smooth function, such a point could only be the equilibrium point V^{eq} which would remain constant in time. Hence all scalar relaxation ODEs are monotonic, and (14), being a special case of (12), is a *necessary* condition for (8) to be a relaxation ODE.

Now if the initial condition V_0 is given as $V_0 = V^{\mathrm{eq}}$, then $S(V_0) = 0$ and (9) holds trivially. Otherwise, for any δ satisfying

$$0 < \delta < |V^{\mathrm{eq}} - V_0|, \tag{15}$$

we define

$$\mathcal{W} = \left[\min(V_0, V^{\mathrm{eq}} + \delta), \max(V^{\mathrm{eq}} - \delta, V_0)\right], \tag{16}$$

$$C = \min_{V \in \mathcal{W}} |S(V)|. \tag{17}$$

It follows from (14) that C^{-1} is a finite number, and that

$$|V(t > T) - V^{\mathrm{eq}}| < \delta \tag{18}$$

where T is given by

$$T = \frac{|V^{\mathrm{eq}} - V_0|}{C}\epsilon. \tag{19}$$

Hence (9) holds, and (14) is also a *sufficient* condition for (8) to be a relaxation ODE in the scalar case. □

If the relaxation processes are fully independent, this property will carry directly over to systems. For instance, the relaxation part of the five-equation two-phase flow model investigated by Munkejord [20], describing simultaneous volume and momentum transfer, consists of independent relaxation processes and is monotonic in the sense of Definition 2.

Remark 1. *A simple example of a coupled, nonlinear and globally monotonic relaxation system can be constructed as follows:*

$$\boldsymbol{V} = \begin{bmatrix} v_1 \\ v_2 \end{bmatrix}, \qquad \boldsymbol{S}(\boldsymbol{V}) = \begin{bmatrix} \left(\alpha_1 + \beta_1 v_2^2\right) v_1 \\ \left(\alpha_2 + \beta_2 v_1^2\right) v_2 \end{bmatrix}, \tag{20}$$

where

$$\boldsymbol{V}^{\mathrm{eq}} = \begin{bmatrix} 0 \\ 0 \end{bmatrix} \tag{21}$$

and

$$\alpha_i, \beta_i < 0 \quad \forall i \in \{1, 2\}. \tag{22}$$

This is however a theoretical example, and monotonicity may easily be lost for strongly coupled relaxation systems of practical interest. Consequently, one should be aware that the methods presented in this paper are fully general only for the scalar case, yet also applicable to a limited class of coupled systems.

3.2. **A Strong Stability Requirement.** An essential property of monotonic relaxation systems is that the solution vector remains bounded by the equilibrium value at all times. To avoid unphysical solutions and numerical oscillations, we want our numerical method to possess an analogous property.

Definition 3. *Consider a monotonic relaxation ODE with initial conditions $\boldsymbol{V}^n$ and equilibrium point $\boldsymbol{V}^{\mathrm{eq}}$. Let the numerical solution be given through some operator $\mathcal{S}(\Delta t)$ as*

$$\boldsymbol{V}^{n+1} = \mathcal{S}(\Delta t)\boldsymbol{V}^n. \tag{23}$$

The operator $\mathcal{S}$ will be denoted as **monotonically asymptotically stable** *if it satisfies the following properties.*

MA1: *The operator is* **consistent** *with the relaxation system to be solved, i.e. the local truncation error is of at least second order in Δt.*

MA2: *The solution is unconditionally* **bounded** *by the equilibrium value, i.e.*

$$\begin{aligned} V_i^{n+1} &\in (V_i^n, V_i^{\mathrm{eq}}) \qquad \textit{for} \quad V_i^n < V_i^{\mathrm{eq}}, \\ V_i^{n+1} &= V_i^n \qquad\qquad \textit{for} \quad V_i^n = V_i^{\mathrm{eq}}, \\ V_i^{n+1} &\in (V_i^{\mathrm{eq}}, V_i^n) \qquad \textit{for} \quad V_i^n > V_i^{\mathrm{eq}} \end{aligned} \tag{24}$$

for all $i \in \{1, \ldots, N\}$ *and for all* Δt.

Common explicit methods typically do not possess this form of stability. For instance, the forward Euler method satisfies the property MA2 only conditionally, with a strong restriction on the time step:

$$\frac{\Delta t}{\epsilon} < \min_i \left(\frac{V_i^{\mathrm{eq}} - V_i^n}{S_i(\boldsymbol{V}^n)} \right). \tag{25}$$

Implicit methods may however possess such strong stability, as exemplified as follows.

Proposition 2. *The backward Euler method, defined by*

$$\boldsymbol{V}^{n+1} = \boldsymbol{V}^n + \frac{\Delta t}{\epsilon} \boldsymbol{S}(\boldsymbol{V}^{n+1}), \tag{26}$$

is monotonically asymptotically stable in the sense of Definition 3.

Proof. It is well known and easy to check that the backward Euler method is consistent; i.e. the property MA1 is satisfied. We now prove the property MA2 by showing that we otherwise get contradictions. First, we note that the backward Euler method preserves the equilibrium point. We now consider the case $V_i^{\mathrm{eq}} > V_i^n$. Assume that the solution $\boldsymbol{V}^{n+1}$ of (26) satisfies

$$V_i^{n+1} < V_i^n. \tag{27}$$

From (12), we then have $S_i(\boldsymbol{V}^{n+1}) > 0$ which inserted into (26) yields $V_i^{n+1} > V_i^n$, in contradiction to (27).

Similarly, assume that the solution $\boldsymbol{V}^{n+1}$ of (26) satisfies

$$V_i^{n+1} > V_i^n. \tag{28}$$

From (12), we then have $S_i(\boldsymbol{V}^{n+1}) < 0$ which inserted into (26) yields $V_i^{n+1} < V_i^n$, in contradiction to (28).

The same steps will prove the remaining case $V_i^{\mathrm{eq}} < V_i^n$. □

Implicit methods generally require the solution of a system of nonlinear equations, which raises its own computational efficiency and robustness issues. This motivates the *explicit* monotonically asymptotically stable method presented in the following.

Definition 4. *The numerical method given by*

$$V_i^{n+1} = V_i^n + (V_i^{\mathrm{eq}} - V_i^n) \left(1 - \exp\left(-\frac{\Delta t}{\tau_i} \right) \right), \tag{29}$$

where

$$\tau_i = \epsilon \frac{V_i^{\mathrm{eq}} - V_i^n}{S_i(\boldsymbol{V}^n)}, \tag{30}$$

will be denoted as the **ASY1** *method.*

Proposition 3. *The ASY1 method is monotonically asymptotically stable in the sense of Definition 3.*

Proof. Assume first that $V_i^{\mathrm{eq}} \neq V_i^n$. Taylor-expanding (29) shows that the method is consistent to first order with (8). Note also that (29) satisfies

$$\lim_{V_i^n \to V_i^{\mathrm{eq}}} V_i^{n+1} = V_i^{\mathrm{eq}}, \tag{31}$$

hence the property MA1 is satisfied. From (12) and (30) it also follows that the exponential function is bounded by the interval $(0, 1]$. Hence the property MA2 is satisfied. □

Note that the ASY1 method (29) inserts a numerical "barrier" at the point $V_i = V_i^{\mathrm{eq}}$ through which the solution can never pass. Hence the method cannot be consistent unless this barrier is also present in the underlying mathematical equation, as is the case for monotonic relaxation ODEs.

Otherwise, we will formally lose first-order accuracy at the barrier, as described in the following.

Proposition 4. *When applied to a general ODE*

$$\frac{\mathrm{d}\boldsymbol{V}}{\mathrm{d}t} = \boldsymbol{Q}(\boldsymbol{V}), \tag{32}$$

where $\boldsymbol{Q}(\boldsymbol{V})$ is a smooth function, the method (29)–(30) *is consistent in the limit $V_i^n \to V_i^{\mathrm{eq}}$ only if*

$$Q_i(\boldsymbol{V}) = 0 \quad \textit{for} \quad V_i = V_i^{\mathrm{eq}}. \tag{33}$$

Proof. The local truncation error of the method for the component V_i can be written as

$$T_i(\boldsymbol{V}^n) = \frac{1}{2}(\Delta t)^2 \left(Q_i(\boldsymbol{V}^n) \left(\frac{\partial Q_i}{\partial V_i} + \frac{Q_i(\boldsymbol{V}^n)}{V_i^{\mathrm{eq}} - V_i^n} \right) + \sum_{k \neq i} \frac{\partial Q_i}{\partial V_k} Q_k(\boldsymbol{V}^n) \right) + \mathcal{O}(\Delta t^3). \tag{34}$$

Now if (33) holds, we obtain

$$\lim_{V_i^n \to V_i^{\mathrm{eq}}} \frac{\partial Q_i}{\partial V_k} = 0 \quad \forall k \neq i, \tag{35}$$

and also

$$\lim_{V_i^n \to V_i^{\mathrm{eq}}} T_i(\boldsymbol{V}^n) = 0. \tag{36}$$

However, if (33) does *not* hold, the second-order coefficient diverges and the local truncation error degenerates to

$$T_i(\boldsymbol{V}^n) \sim \mathcal{O}(\Delta t). \tag{37}$$

□

The notion of *monotonic asymptotic* stability may be interpreted as a *dual* consistency principle; consistency in the large (MA2) and the small (MA1), or the stiff and non-stiff limit of the time step.

3.3. **Accuracy Near Equilibrium.** The exponential function employed in (29) is of course only one of many functions that asymptotically approaches a limit value. However, it becomes the natural choice as it corresponds to the *exact* solution for linear monotonic relaxation problems. In this respect, it is worth noting that solutions to relaxation systems in the form (1) tend to remain close to equilibrium. We have the following proposition.

Proposition 5. *When applied to a monotonic relaxation ODE, the ASY1 method is exact to first-order perturbations to the equilibrium state. More precisely, if we write*

$$\boldsymbol{V}^n = \boldsymbol{V}^{\mathrm{eq}} + \delta\tilde{\boldsymbol{V}}, \tag{38}$$

then for all $\Delta t \geq 0$ *the numerical solution* (29) *satisfies*

$$V_i(t^n + \Delta t) - V_i^{n+1} = \mathcal{O}(\delta^2) \quad \forall i, \tag{39}$$

where $\boldsymbol{V}(t)$ *is the exact solution.*

Proof. It follows from monotonicity that

$$V_i(t) - V_i^{\mathrm{eq}} \sim \mathcal{O}(\delta) \quad \forall i. \tag{40}$$

Consequently, we may expand the source term as

$$S_i(\boldsymbol{V}(t)) = S_i(\boldsymbol{V}^{\mathrm{eq}}) + \sum_{k=1}^{N} \frac{\partial S_i}{\partial V_k} \left(V_k(t) - V_k^{\mathrm{eq}}\right) + \mathcal{O}(\delta^2). \tag{41}$$

By definition a monotonic relaxation ODE satisfies

$$S_i(\boldsymbol{V}) = 0 \quad \text{for} \quad V_i = V_i^{\mathrm{eq}}, \tag{42}$$

hence

$$\frac{\partial S_i}{\partial V_k} = 0 \quad \text{for} \quad k \neq i \tag{43}$$

at the point $\boldsymbol{V}^{\mathrm{eq}}$, and (41) reduces to

$$S_i(\boldsymbol{V}(t)) = \frac{\partial S_i}{\partial V_i} \left(V_i(t) - V_i^{\mathrm{eq}}\right) + \mathcal{O}(\delta^2). \tag{44}$$

As this holds for all t, we may write

$$S_i(\boldsymbol{V}(t)) = S_i(\boldsymbol{V}^n) \frac{V_i^{\mathrm{eq}} - V_i(t)}{V_i^{\mathrm{eq}} - V_i^n} + \mathcal{O}(\delta^2), \tag{45}$$

and using (8) we obtain

$$\epsilon \frac{V_i^{\mathrm{eq}} - V_i^n}{S_i(\boldsymbol{V}^n)} \frac{\mathrm{d}V_i(t)}{V_i^{\mathrm{eq}} - V_i(t)} = (1 + \mathcal{O}(\delta))\,\mathrm{d}t, \tag{46}$$

where we have used that

$$S_i(\boldsymbol{V}^n) \sim \mathcal{O}(\delta) \quad \forall i. \tag{47}$$

Integrating (46) we obtain

$$\frac{V_i^{\mathrm{eq}} - V_i(t + \Delta t)}{V_i^{\mathrm{eq}} - V_i^n} = \exp\left(-\frac{S_i(\boldsymbol{V}^n)\Delta t}{\epsilon(V_i^{\mathrm{eq}} - V_i^n)}\right) + \mathcal{O}(\delta), \tag{48}$$

which can be rewritten as

$$V_i(t + \Delta t) = V_i^n + (V_i^{\mathrm{eq}} - V_i^n)\left(1 - \exp\left(-\frac{S_i(\boldsymbol{V}^n)\Delta t}{\epsilon(V_i^{\mathrm{eq}} - V_i^n)}\right)\right) + \mathcal{O}(\delta^2). \tag{49}$$

We now recover (39) by using (29)–(30). □

3.4. **Second-Order Accuracy.** A general explicit two-stage Runge–Kutta scheme for the ODE (8) can be written in the form

$$\boldsymbol{V}^* = \boldsymbol{V}^n + a\frac{\Delta t}{\epsilon}\boldsymbol{S}(\boldsymbol{V}^n) \tag{50}$$

$$\boldsymbol{V}^{n+1} = \boldsymbol{V}^n + \frac{\Delta t}{\epsilon}\left(b_1\boldsymbol{S}(\boldsymbol{V}^n) + b_2\boldsymbol{S}(\boldsymbol{V}^*)\right), \tag{51}$$

where for second-order accuracy the parameters a, b_1 and b_2 must satisfy (see for instance [16, Ch. 8]):

$$b_1 + b_2 = 1, \qquad ab_2 = \frac{1}{2}. \tag{52}$$

In this section, we make some preliminary investigations into higher-order versions of the ASY method by devising a similar two-stage application of (29).

Definition 5. *The numerical method given by*

$$V_i^* = V_i^n + (V_i^{\mathrm{eq}} - V_i^n)\left(1 - \exp\left(-a\frac{\Delta t}{\tau_i}\right)\right) \tag{53}$$

$$V_i^{n+1} = V_i^n + (V_i^{\mathrm{eq}} - V_i^n)\left(1 - b_1\exp\left(-\frac{\Delta t}{\tau_i}\right) - b_2\exp\left(-\frac{\Delta t}{\tau_i^*}\right)\right), \tag{54}$$

where

$$\tau_i = \epsilon\frac{V_i^{\mathrm{eq}} - V_i^n}{S_i(\boldsymbol{V}^n)}, \qquad \tau_i^* = \epsilon\frac{V_i^{\mathrm{eq}} - V_i^*}{S_i(\boldsymbol{V}^*)}, \tag{55}$$

and the parameters a, b_1 and b_2 satisfy

$$b_1 + b_2 = 1, \qquad ab_2 = \frac{1}{2}, \tag{56}$$

as well as

$$b_2 \in (0, 1], \tag{57}$$

will be denoted as the **ASY2** *method.*

Proposition 6. *The ASY2 method is second-order accurate in Δt when applied to a monotonic relaxation ODE.*

Proof. Expanding τ_i^* we obtain

$$\frac{1}{\tau_i^*} = \frac{1}{\tau_i}\left(1 + a\Delta t\left(\frac{1}{\tau_i} + \frac{1}{S_i(\boldsymbol{V}^n)}\sum_{k=1}^{N}\frac{\partial S_i}{\partial V_k}\frac{S_k(\boldsymbol{V}^n)}{\epsilon}\right)\right) + \mathcal{O}(\Delta t^2), \tag{58}$$

where have used that

$$V_i^* = V_i^n + a\frac{\Delta t}{\epsilon}S_i(\boldsymbol{V}^n) + \mathcal{O}(\Delta t^2), \tag{59}$$

$$S_i(\boldsymbol{V}^*) = S_i(\boldsymbol{V}^n) + a\frac{\Delta t}{\epsilon}\sum_{k=1}^{N}\frac{\partial S_i}{\partial V_k}S_k(\boldsymbol{V}^n) + \mathcal{O}(\Delta t^2). \tag{60}$$

Substituting (58) into (54) and expanding the exponential function we obtain

$$\begin{aligned} V_i^{n+1} &= V_i^n + \frac{\Delta t}{\epsilon}S_i(\boldsymbol{V}^n)\left(b_1 + b_2\right) \\ &+ \frac{1}{2}\frac{\Delta t^2}{\epsilon^2}\left((2ab_2 - b_1 - b_2)\frac{S_i(\boldsymbol{V}^n)^2}{V_i^{\mathrm{eq}} - V_i^n} + 2ab_2\sum_{k=1}^{N}\frac{\partial S_i}{\partial V_k}S_k(\boldsymbol{V}^n)\right) + \mathcal{O}(\Delta t^3), \end{aligned} \tag{61}$$

whereas the exact solution satisfies

$$V_i(t^n + \Delta t) = V_i^n + \frac{\Delta t}{\epsilon} S_i(\boldsymbol{V}^n) + \frac{1}{2}\frac{\Delta t^2}{\epsilon^2} \sum_{k=1}^{N} \frac{\partial S_i}{\partial V_k} S_k(\boldsymbol{V}^n) + \mathcal{O}(\Delta t^3). \tag{62}$$

Now using (56) we may write

$$V_i(t^n + \Delta t) - V_i^{n+1} = \mathcal{O}(\Delta t^3) \quad \forall V_i^n \neq V_i^{\mathrm{eq}}. \tag{63}$$

We finally observe that ASY2 method respects the limit

$$\lim_{V_i^n \to V_i^{\mathrm{eq}}} V_i^{n+1} = V_i^{\mathrm{eq}}. \tag{64}$$

□

Proposition 7. *The ASY2 method is monotonically asymptotically stable in the sense of Definition 3.*

Proof. The property MA1 follows immediately from Proposition 6. From (12), it follows that the exponential functions of (54) are bounded by the interval $(0, 1]$. The property MA2 then follows from (56)–(57). □

As might be expected, Proposition 5 also naturally extends to the ASY2 method.

Proposition 8. *When applied to a monotonic relaxation ODE, the ASY2 method is exact to first-order perturbations to the equilibrium state. More precisely, if we write*

$$\boldsymbol{V}^n = \boldsymbol{V}^{\mathrm{eq}} + \delta \tilde{\boldsymbol{V}}, \tag{65}$$

then for all $\Delta t \geq 0$ the numerical solution (53)–(54) satisfies

$$V_i(t^n + \Delta t) - V_i^{n+1} = \mathcal{O}(\delta^2) \quad \forall i, \tag{66}$$

where $\boldsymbol{V}(t)$ is the exact solution.

Proof. We have

$$S_i(\boldsymbol{V}^*) = \frac{\partial S_i}{\partial V_i} (V_i^* - V_i^{\mathrm{eq}}) + \mathcal{O}(\delta^2), \tag{67}$$

hence from (55) we obtain

$$\frac{1}{\tau_i^*} = \frac{1}{\tau_i} + \mathcal{O}(\delta^2). \tag{68}$$

Using (56), we may then write (54) as

$$\begin{aligned} V_i^{n+1} &= V_i^n + (V_i^{\mathrm{eq}} - V_i^n) \left(1 - \exp\left(-\frac{\Delta t}{\tau_i}\right) \left(b_1 + b_2(1 + \mathcal{O}(\delta^2))\right)\right) \\ &= V_i^n + (V_i^{\mathrm{eq}} - V_i^n) \left(1 - \exp\left(-\frac{\Delta t}{\tau_i}\right)\right) + \mathcal{O}(\delta^3). \end{aligned} \tag{69}$$

In other words, ASY1 and ASY2 coincide to second order in perturbations to the equilibrium state. The result then follows directly from Proposition 5. □

4. A Granular-Gas Flow Model

Granular gases have lately been the subject of considerable theoretical, numerical and experimental studies [9, 24, 23, 27, 25]. In this work we consider a continuum model for granular-gas flow, in which the dynamics are accounted for by a hyperbolic conservation law with relaxation. In addition to having been previously studied in the literature, this model is suitable for our current purposes for the following reasons.

- The relaxation part of the system is a monotonic nonlinear relaxation ODE.
- The equilibrium state corresponds to a granular temperature $T = 0$ and is hence easy to calculate.
- Numerically overshooting the equilibrium would be undesirable, as it would lead to the unphysical state $T < 0$.

4.1. **Fluid-Mechanical Equations.** The dynamics of a one-dimensional granular-gas flow under the influence of gravity, in the form considered by Serna and Marquina [27], can be described by the Euler-like equations

$$\frac{\partial \rho}{\partial t} + \frac{\partial (\rho u)}{\partial x} = 0, \tag{70a}$$

$$\frac{\partial (\rho u)}{\partial t} + \frac{\partial (\rho u^2 + p)}{\partial x} = \rho g, \tag{70b}$$

$$\frac{\partial E}{\partial t} + \frac{\partial\, u(E + p)}{\partial x} = \Theta + \rho g u. \tag{70c}$$

In the above, ρ is the density, u is the velocity, p is the pressure, g is the gravitational acceleration, E is the energy density and Θ is the rate of energy loss due to inelastic collisions. The energy density consists of both kinetic and internal energy and is given by $E = (1/2)\rho u^2 + (3/2)\rho T$, where T is the granular temperature.

Following Serna and Marquina [27], we use an energy-loss term based on Haff's cooling law [10], given by

$$\Theta(\rho, T) = -\frac{12}{\sqrt{\pi}} \frac{1 - e^2}{\sigma} \rho T^{3/2} G(\nu), \tag{71}$$

where σ is the particle diameter and $e \in [0, 1]$ is the restitution coefficient. For $e = 1$ we recover a fully elastic model. The statistical correlation function $G(\nu)$ is given by

$$G(\nu) = \nu \left(1 - \left(\frac{\nu}{\nu_M} \right)^{\frac{3}{4}\nu_M} \right)^{-1}, \tag{72}$$

where $\nu = (\pi/6)\rho\sigma^3$ is the volume fraction and ν_M is the maximal volume fraction.

The pressure is determined by a granular equation of state (EOS), introduced by Goldshtein and Shapiro [9], given by

$$p(\rho, T) = T\rho(1 + 2(1 + e)G(\nu)). \tag{73}$$

4.2. **The Relaxation ODE.** Within the splitting (2a)–(2b), we obtain

$$\boldsymbol{U} = \begin{bmatrix} \rho \\ \rho u \\ E \end{bmatrix} \qquad \text{and} \qquad \frac{1}{\epsilon} \boldsymbol{R}(\boldsymbol{U}) = \begin{bmatrix} 0 \\ 0 \\ \Theta(\rho, T) \end{bmatrix}. \tag{74}$$

For any initial condition

$$\boldsymbol{U}_0 = \begin{bmatrix} \rho_0 \\ \rho_0 u_0 \\ E_0 \end{bmatrix}, \tag{75}$$

this may be written in the reduced form (8) with

$$V(\boldsymbol{U}) = E, \tag{76}$$

$$\frac{1}{\epsilon} S(V) = -\frac{4}{\sqrt{3\pi}} \frac{1-e^2}{\sigma} \rho_0 \left(2\frac{V}{\rho_0} - u^2 \right)^{3/2} G(\nu_0). \tag{77}$$

Furthermore, for any V we can reconstruct the full state vector $\boldsymbol{U}$ as

$$\boldsymbol{U}(V) = \begin{bmatrix} \rho_0 \\ \rho_0 u_0 \\ V \end{bmatrix}. \tag{78}$$

5. Numerical Tests

5.1. **Verification of the Order of Convergence.** The purpose of this section is to numerically verify the order of convergence of the monotonically asymptotically stable integrators presented in Section 3. Specifically, we wish to verify that the ASY1 scheme (29) is first-order accurate and that the ASY2 scheme (53)–(54) is second-order accurate. The two-stage ASY2 scheme is completely determined by the parameter a in the order conditions (56). For the calculations of this paper, we choose the parameter $a = 1$. By this choice, we only need two evaluations of the exponential function in (53)–(54).

We consider an initial value problem, based on the scalar relaxation ODE of the granular-gas model, given by

$$\frac{\partial E(t)}{\partial t} = -\frac{4}{\sqrt{3\pi}} \frac{1-e^2}{\sigma} \rho_0 \left(2\frac{E(t)}{\rho_0} - u_0^2 \right)^{3/2} G(\rho_0), \quad E(0) = E_0. \tag{79}$$

For this numerical test we use $e = 0.97$, $\sigma = 10^{-3}\,\mathrm{m}$, $\rho_0 = 10.0\,\mathrm{kg/m^3}$ and $u_0 = 18.0\,\mathrm{m/s}$. The initial energy is given by

$$E_0 = 3966.5\,\mathrm{J/m^3}, \tag{80}$$

and the corresponding equilibrium energy is $E^{\mathrm{eq}} = (1/2)\rho_0 u_0^2 = 1620.0\,\mathrm{J/m^3}$.

A reference solution $E_{\mathrm{ref}}(1.0)$ was calculated using the second-order modified Euler scheme with a step size $\Delta t = 2^{-20}\,\mathrm{s}$. The modified Euler scheme is given by the two-step explicit Runge–Kutta method (50)–(51) with $a = 0.5$. In order to estimate the order of convergence we calculate the error $\mathcal{E} = |E_{\mathrm{ref}}(1.0) - \hat{E}(1.0)|$ for numerical solutions $\hat{E}$, using different step sizes. Let $\mathcal{E}^i$ be the error using step-size $\Delta t_i = 2^{-i}$, for $i \in \mathbb{N}$. For sufficiently small Δt, the order of convergence n is then given by

$$n = \log_2 \left(\frac{\mathcal{E}^{i-1}}{\mathcal{E}^i} \right). \tag{81}$$

Table 1 shows the error and the estimated order of convergence for the ASY1 scheme. The results are consistent with a first-order solver.

Table 2 shows the error and estimated order of convergence for the ASY2 scheme. These results agree with this being a second-order accurate scheme.

TABLE 1. The error $\mathcal{E} = |E_{\text{ref}}(1.0) - \hat{E}(1.0)|$ in the numerical solution at $t = 1.0\,\text{s}$ using the ASY1 scheme, for different values of the step-size Δt. The number n indicates the estimated order of convergence.

Δt	$\mathcal{E}^i$	$\mathcal{E}^{i-1}/\mathcal{E}^i$	n
2^{-2}	4.02869674	-	-
2^{-3}	1.99680512	2.0176	1.0126
2^{-4}	0.99408608	2.0087	1.0063
2^{-5}	0.49597241	2.0043	1.0031
2^{-6}	0.24771960	2.0022	1.0016
2^{-7}	0.12379328	2.0011	1.0008
2^{-8}	0.06188003	2.0005	1.0004
2^{-9}	0.03093586	2.0003	1.0002
2^{-10}	0.01546689	2.0001	1.0001

TABLE 2. The error $\mathcal{E} = |E_{\text{ref}}(1.0) - \hat{E}(1.0)|$ in the numerical solution at $t = 1.0\,\text{s}$ using the ASY2 scheme, for different values of the step-size Δt. The number n indicates the estimated order of convergence.

Δt	$\mathcal{E}^i$	$\mathcal{E}^{i-1}/\mathcal{E}^i$	n
2^{-2}	0.01629915	-	-
2^{-3}	0.00393750	4.1395	2.0494
2^{-4}	0.00096757	4.0695	2.0248
2^{-5}	0.00023981	4.0347	2.0125
2^{-6}	0.00005969	4.0173	2.0062
2^{-7}	0.00001489	4.0086	2.0031
2^{-8}	0.00000372	4.0041	2.0015
2^{-9}	0.00000093	4.0014	2.0005
2^{-10}	0.00000023	3.9982	1.9993

5.2. **Numerical Method.** In order to numerically test the ASY methods on the granular-gas model described in Section 4, we use a fractional-step method as described in Section 2.1. This means that we need a numerical solver for the hyperbolic part (2a) to use in tandem with the exponential integrator.

5.2.1. *A Multi-Stage Scheme.* We consider a uniform grid in space and time, and denote $t^n = t_0 + n\,\Delta t$ and $x_j = x_0 + j\,\Delta x$. For a first-order accurate numerical scheme, we advance the solution $\boldsymbol{U}_j^n$ forward in time by using

$$\boldsymbol{U}_j^{n+1} = \boldsymbol{U}_j^n + \mathcal{F}_j^n \Delta t, \tag{82}$$

where

$$\mathcal{F}_j^n = \frac{1}{\Delta x}\left(\boldsymbol{F}_{j-1/2}^n - \boldsymbol{F}_{j+1/2}^n\right) + \boldsymbol{\mathcal{Q}}(\boldsymbol{U}_j^n). \tag{83}$$

In the above, $\boldsymbol{F}_{j+1/2}^n$ is the numerical approximation to the inter-cell flux and $\boldsymbol{\mathcal{Q}}(\boldsymbol{U}_j^n)$ are local source terms other than relaxation terms. For the granular-gas model, $\boldsymbol{\mathcal{Q}}(\boldsymbol{U})$ will be the gravity source terms.

In the Multi-Stage (MUSTA) approach, the inter-cell flux is calculated by solving the local Riemann problem at each cell interface on a local grid [29]. The solution on the local grid is then advanced in several stages giving an approximation to the inter-cell flux. In our application, we will use four local grid cells and two local iteration steps. The CFL number of the local grid is kept the same as on the global grid.

5.2.2. *High Resolution.* In a high resolution (second order) extension to the MUSTA scheme, we employ a second-order strong-stability-preserving (SSP) Runge–Kutta method to advance the solution forward in time. The two-stage scheme is given by

$$\begin{aligned} \boldsymbol{U}_j^* &= \boldsymbol{U}_j^n + \mathcal{F}_j^n \Delta t, \\ \boldsymbol{U}_j^{n+1} &= \frac{1}{2}\boldsymbol{U}_j^n + \frac{1}{2}\boldsymbol{U}_j^* + \frac{1}{2}\mathcal{F}_j^* \Delta t. \end{aligned} \tag{84}$$

In order to obtain second-order accuracy in space, a piecewise linear MUSCL interpolation [22, 30] was used. For the granular-gas model, the variables used in the interpolation were given by

$$\boldsymbol{W} = \begin{bmatrix} \rho & v & p \end{bmatrix}^T. \tag{85}$$

We reconstruct these variables to the right and to the left of the cell interface as

$$\boldsymbol{W}_{j+1/2}^{\mathrm{R}} = \boldsymbol{W}_{j+1} - \frac{\Delta x}{2}\boldsymbol{\sigma}_{j+1} \quad \text{and} \quad \boldsymbol{W}_{j+1/2}^{\mathrm{L}} = \boldsymbol{W}_{j} + \frac{\Delta x}{2}\boldsymbol{\sigma}_{j}, \tag{86}$$

respectively. The cell slopes $\boldsymbol{\sigma}_j$ are calculated using a *minmod* slope, given by

$$\sigma_{j,i} = \operatorname{minmod}\left(\frac{W_{j,i} - W_{j-1,i}}{\Delta x}, \frac{W_{j+1,i} - W_{j,i}}{\Delta x}\right), \tag{87}$$

where the minmod function is defined as

$$\operatorname{minmod}(a,b) = \begin{cases} 0 & \text{if } ab \le 0 \\ a & \text{if } |a| < |b| \text{ and } ab > 0 \\ b & \text{if } |b| < |a| \text{ and } ab > 0 \end{cases}. \tag{88}$$

The reconstructed values at the interface are then used for the Riemann problem on the local MUSTA grid, in order to obtain second-order accuracy in space. We refer to the high-resolution scheme as MUSCL-MUSTA.

5.3. **Case: Granular-Gas Tube.** In this section we use the ASY integrators as a part of a fractional-step method in order to compare with previously reported results for the granular-gas model.

We consider the case of a granular gas in a vertical tube hitting a solid wall at the bottom end, as used by Serna and Marquina [27] and also Pareschi and Russo [23]. The 0.1 m tube is initially filled with a granular gas with volume fraction $\nu = 0.018$, velocity 0.18 m/s and pressure $p = 1589.26$ Pa. We use the gravitational acceleration $g = 9.8$ m/s, the restitution coefficient $e = 0.97$, the maximum volume fraction $\nu_M = 0.65$ and the particle diameter $\sigma = 10^{-3}$ m. The left boundary condition is given by an incoming flow consistent with the initial condition. At the right end of the domain we used a reflective boundary condition.

Simulations were carried out using 200 computational cells and a CFL number of 0.4. Figure 1 shows the results for the volume fraction, granular temperature and velocity at $t = 0.23$ s, using the MUSTA-ASY1 scheme with Godunov splitting and

the MUSCL-MUSTA-ASY2 scheme with Strang splitting. The reference solution was computed using the MUSCL-MUSTA-ASY2 scheme with 10 000 cells.

The results show a shock being formed when the gas hits the solid wall. The shock propagates backwards and the gas continues to compress against the wall until the maximum volume fraction is reached at the right boundary. It is also at the right boundary the difference between the first and second-order schemes is most prominent, as illustrated in Figure 2. For the second-order MUSCL-MUSTA-ASY2 scheme some spurious oscillations can be observed near the shock, these are associated with the MUSCL interpolation in the hyperbolic step.

Our results do not compare unfavourably to those previously reported [23, 27] in terms of accuracy and numerical robustness.

6. Summary

We have investigated a technique, based on exponential integration, for solving monotonic relaxation ODEs. First and second-order versions of the method have been presented. We have proved that the resulting methods possess desirable accuracy and stability properties. In particular, for first-order corrections to the equilibrium value, the methods yield the exact solution. Furthermore, the methods yield numerical solutions that are unconditionally bounded by the equilibrium state.

Through operator splitting, we have applied the methods to a system of hyperbolic conservation laws with relaxation, representing flow of granular gases. The simulations indicate that the currently selected approach, based on MUSCL interpolation in the hyperbolic step, is comparable to previously published results in terms of accuracy and appearance of numerical oscillations.

In summary, we have analytically demonstrated beneficial properties of the methods in the stiff and non-stiff limits of the time step. Our numerical experiments further verify the applicability of the methods for intermediate time steps. Hence the approach shows promise for solving hyperbolic relaxation processes where robustness in the relaxation step is essential, for instance to avoid vacuum or negative-temperature states.

Further work includes deriving higher-order conditions for general multi-stage versions of the method. In this context, it would also be of interest to derive unsplit versions of the approach, following for instance the ideas of Jin [15]. An extension to more general systems, through the matrix exponential, should also be investigated.

Acknowledgements

The work of the second author was supported by A/S Norske Shell. The remaining authors were financed through the CO_2 Dynamics project. These authors acknowledge the support from the Research Council of Norway (189978), Gassco AS, Statoil Petroleum AS and Vattenfall AB.

References

[1] H. Berland, B. Owren and B. Skaflestad, *B*-series and order conditions for exponential integrators, *SIAM J. Numer. Anal.* **43**, 1715–1727, (2005).

[2] S. Boscarino, Error analysis of IMEX Runge-Kutta methods derived from differential-algebraic systems, *SIAM J. Numer. Anal.* **45**, 1600–1621, (2007).

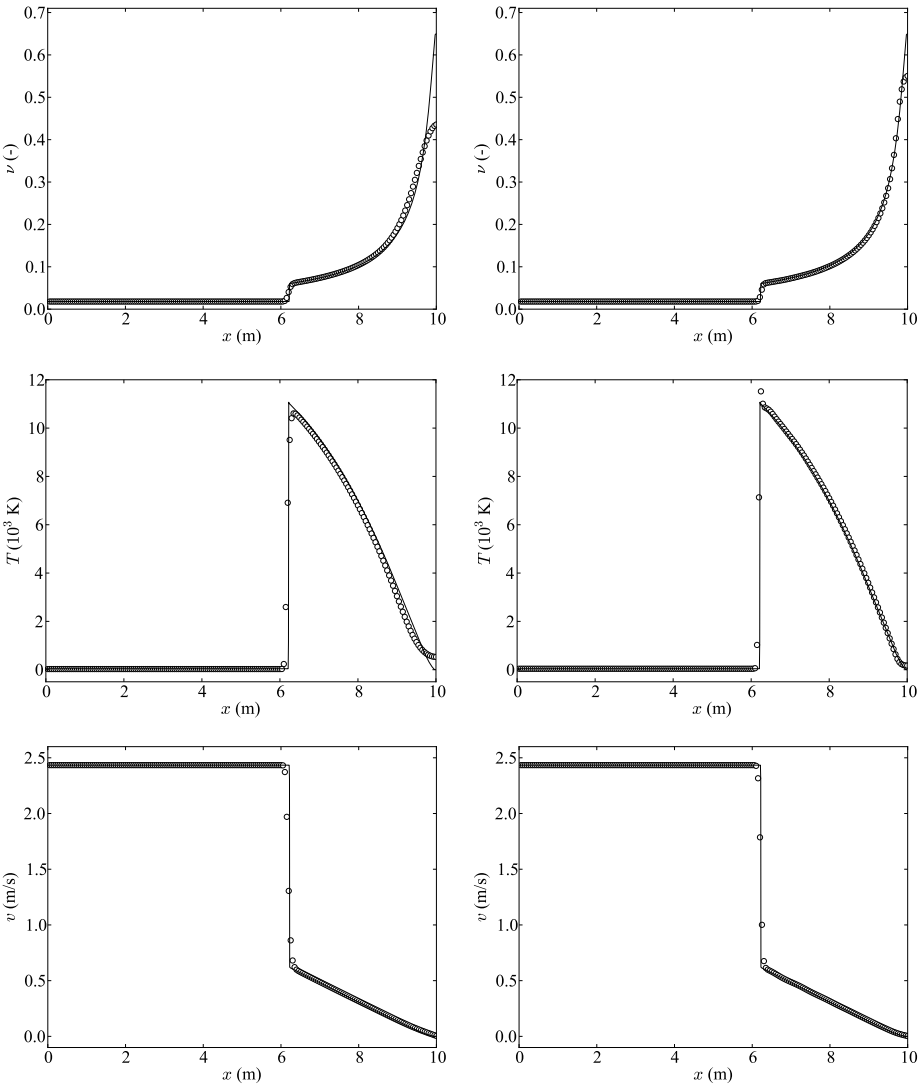

(a) MUSTA-ASY1 (b) MUSCL-MUSTA-ASY2

FIGURE 1. Granular-gas shock case at $t = 0.23\,\mathrm{s}$ for the MUSTA-ASY1 scheme and the MUSCL-MUSTA-ASY2 scheme. The solid line is the reference solution.

[3] S. Boscarino and G. Russo, On a class of uniformly accurate IMEX Runge-Kutta schemes and applications to hyperbolic systems with relaxation, *SIAM J. Sci. Comput.* **31**, 1926–1945, (2009).

[4] G.-Q. Chen, C. D. Levermore and T.-P. Liu, Hyperbolic conservation laws with stiff relaxation terms and entropy, *Comm. Pure Appl. Math.* **47**, 787–830, (1994).

[5] S. M. Cox and P. C. Matthews, Exponential time differencing for stiff systems, *J. Comput. Phys.* **176**, 430–455, (2002).

[6] B. H. Ehle and J. D. Lawson, Generalized Runge-Kutta processes for stiff initial-value problems, *J. Inst. Maths. Applics* **16**, 11–21, (1975).

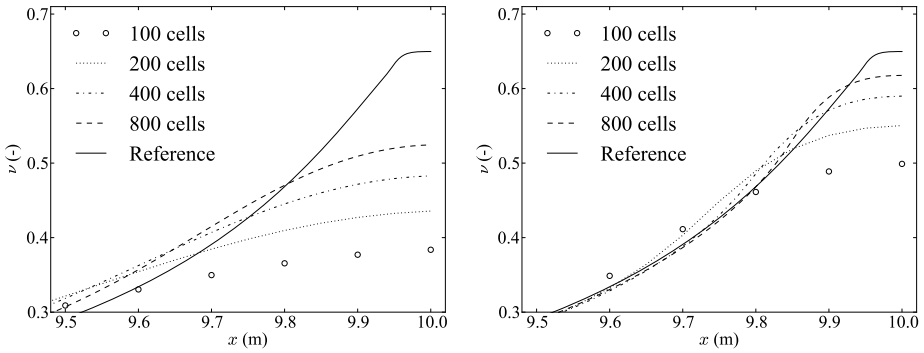

(a) MUSTA-ASY1 (b) MUSCL-MUSTA-ASY2

FIGURE 2. Convergence under grid refinement at the right boundary at $t = 0.23\,\mathrm{s}$.

[7] T. Flåtten and H. Lund, Relaxation two-phase flow models and the subcharacteristic condition, *Math. Mod. Meth. Appl. S.*, accepted for publication.

[8] T. Flåtten, A. Morin and S. T. Munkejord, Wave propagation in multicomponent flow models, *SIAM J. Appl. Math.* **70**, 2861–2882, (2010).

[9] A. Goldshtein and M. Shapiro, Mechanics of collisional motion of granular materials: Part 1. General hydrodynamic equations, *J. Fluid Mech.* **282**, 75–114, (1995).

[10] P.K. Haff, Grain flow as a fluid mechanical phenomenon, *J. Fluid Mech.* **134**, 401–430, (1983).

[11] M. Hochbruck, C. Lubich and H. Selhofer, Exponential integrators for large systems of differential equations, *SIAM J. Sci. Comput.* **19**, 1552–1574, (1998).

[12] M. Hochbruck and A. Ostermann, Explicit exponential Runge-Kutta methods for semilinear parabolic problems, *SIAM J. Numer. Anal.* **43**, 1069–1090, (2005).

[13] M. Hochbruck, A. Ostermann and J. Schweitzer, Exponential Rosenbrock-type methods, *SIAM. J. Numer. Anal.* **47**, 786–803, (2009).

[14] H. Holden, K. H. Karlsen, K.-A. Lie and N. H. Risebro, *Splitting methods for partial differential equations with rough solutions*, EMS Series of Lectures in Mathematics, EMS Publishing House, Zürich, (2010).

[15] S. Jin, Runge-Kutta methods for hyperbolic conservation laws with stiff relaxation terms, *J. Comput. Phys.* **122**, 51–67, (1995).

[16] D. Kincaid and W. Cheney, *Numerical analysis: mathematics of scientific computing.* American Mathematical Society, Providence, RI, USA, (2009).

[17] S. Krogstad, Generalized integrating factor methods for stiff PDEs, *J. Comput. Phys.* **203**, 72–88, (2005).

[18] J. D. Lawson, Generalized Runge-Kutta processes for stable systems with large Lipschitz constants, *SIAM J. Numer. Anal.* **4**, 372–380, (1967).

[19] T.-P. Liu, Hyperbolic conservation laws with relaxation, *Commun. Math. Phys.* **108**, 153–175, (1987).

[20] S. T. Munkejord, A numerical study of two-fluid models with pressure and velocity relaxation, *Adv. Appl. Math. Mech.* **2**, 131–159, (2010).

[21] R. Natalini, Recent results on hyperbolic relaxation problems. Analysis of systems of conservation laws, in *Chapman & Hall/CRC Monogr. Surv. Pure Appl. Math.*, 99, Chapman & Hall/CRC, Boca Raton, FL, 128–198, (1999).

[22] S. Osher, Convergence of generalized MUSCL schemes, *SIAM J. Numer. Anal.* **22**, 947–961, (1985).

[23] L. Pareschi and G. Russo, Implicit-explicit Runge–Kutta schemes and applications to hyperbolic systems with relaxation, *J. Sci. Comput.* **25**, 129–155, (2005).

[24] M. Pelanti, F. Bouchut and A. Mangeney, A Roe-type scheme for two-phase shallow granular flows over variable topography, *ESAIM: M2AN* **42**, 851–885, (2008).

[25] E. C. Rericha, C. Bizon, M. D. Shattuck and H. L. Swinney, Shocks in supersonic sand, *Phys. Rev. Lett.* **88**, 14302, (2001).
[26] R. Saurel, F. Petitpas and R. Abgrall, Modelling phase transition in metastable liquids: application to cavitating and flashing flows, *J. Fluid Mech.* **607**, 313–350, (2008).
[27] S. Serna and A. Marquina, Capturing shock waves in inelastic granular gases, *J. Comput. Phys.* **209**, 787–795, (2005).
[28] G. Strang, On the construction and comparison of difference schemes, *SIAM J. Numer. Anal.* **5**, 506–517, (1968).
[29] E. F. Toro, MUSTA: A multi-stage numerical flux, *Appl. Numer. Math.* **56**, 1464–1479, (2006).
[30] B. van Leer, Towards the ultimate conservative difference scheme V. A second-order sequel to Godunov's method, *J. Comput. Phys.* **32**, 101–136, (1979).
[31] A. Zein, M. Hantke and G. Warnecke, Modeling phase transition for compressible two-phase flows applied to metastable liquids, *J. Comput. Phys.* **229**, 2964–2998, (2010).